Research on
Engineering
Structures & Materials
journal homepage: http://jresm.org

RESEARCH
GROUP

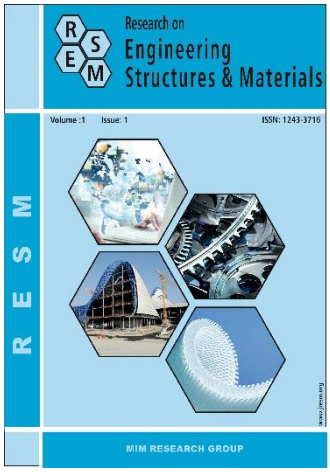

Numerical study of the elasto-plastic buckling in perforated thin steel plates using the constructal design method

Daniel Helbig, Marcelo Langhinrichs Cunha, Caio Cesar Cardoso da Silva, Elizaldo Domingues dos Santos, Ignácio Iturrio, Mauro de Vasconcellos Real, Liércio André Isoldi, Luiz Alberto Oliveira Rocha

Online Publication Date: 25 Jan 2018
URL: http://dx.doi.org/10.17515/resm2017.37ds1123
DOI: http://dx.doi.org/10.17515/resm2017.37ds1123

To cite this article
Helbig O, Cunha ML, Silva CCC, Santos ED, Iturrio I, Real MV, Isoldi LA, Rocha LAO. Numerical study of the elasto-plastic buckling in perforated thin steel plates using the constructal design method. *Res. Eng. Struct. Mat*., 2018; 4(3): 169-187.

Research on Engineering Structures & Materials
journal homepage: http://jresm.org
RESEARCH GROUP

Research Article

Numerical study of the elasto-plastic buckling in perforated thin steel plates using the constructal design method

Daniel Helbig[1], Marcelo Langhinrichs Cunha[2], Caio Cesar Cardoso da Silva[2], Elizaldo Domingues dos Santos[2], Ignácio Iturrioz[1], Mauro de Vasconcellos Real[2], Liércio André Isoldi[*,2], Luiz Alberto Oliveira Rocha[1,3]

[1] *Graduate Program in Mechanical Engineering, Federal University of Rio Grande do Sul - UFRGS, Brazil*
[2] *Graduate Program in Ocean Engineering, Federal University of Rio Grande - FURG, Brazil*
[3] *Graduate Program in Mechanical Engineering, University of Vale do Rio dos Sinos - UNISINOS, Brazil*

Article Info

Article history:
Received 23 Nov 2017
Revised 09 Feb 2018
Accepted 20 Jun 2018

Keywords:

Post-buckling,

Perforated steel plate,

Computational modeling,

Constructal Design method

Abstract

There are several areas of engineering that use thin plates as structural elements, among them, we can highlight their application in the construction of offshore structures, bridges, ship hulls, and aircraft fuselage. In some design situations, the plates may be subjected to compression stresses and, consequently, they may be under the effect of elastic and/or elasto-plastic buckling. The analysis of the buckling phenomenon presents significant differences between one-dimensional elements, such as beams and columns, and two-dimensional elements, such as plates. The buckling phenomenon is directly related to dimensional, constructive and/or operational aspects. In this sense, the presence of perforations in plates causes a redistribution of their stresses, affecting not only their resistance but also their buckling characteristics. In order to solve the problem of elasto-plastic buckling in thin steel plates with perforations, we used computational models developed in Ansys(R) software, which is based on the Finite Element Method (FEM). For the analysis, it was considered perforated plates with constant thickness h for the relationships $H/L = 1.0$ and $H/L = 0.5$, where H is the plate width and L is the plate length. For the volume fraction Φ, i.e., the ratio between the volume of the perforation and the volume of the plate, the following values were considered: 0.08; 0.10; 0.15; 0.20 and 0.25. In addition, the plates were considered to have centralized perforations with the following geometric forms: longitudinal oblong, transverse oblong, elliptic, rectangular, diamond, longitudinal hexagonal, and transverse hexagonal. The shape variation of each perforation type occurs through the ratio H_0/L_0, being H_0 and L_0 the characteristics dimensions of perforation. The Constructal Design method was employed to define the range of possible geometries for the perforated plates, allowing an adequately comparison about the von Mises stress distribution among the studied cases. The results show that the geometric shape variation, for all analyzed perforation types, leads to an optimum geometry.

Introduction

The growing use of the steel plates in structures is directly related to the advantages that this element possesses when compared with other construction types. The high strength of the material to the several stress states, for instance, makes it possible to withstand great internal forces, in spite of having cross-sectional areas relatively small, what turns them lighter [1].

[*]Corresponding author: liercioisoldi@furg.br
DOI: http://dx.doi.org/10.17515/resm2017.37ds1123

As for the thin plates, these are structural elements very used in the naval, aerial, and automotive industries, as well as in the civil construction. It stands out for its use in the construction of shipyards cranes, petroleum platforms, floating docks, ship hulls, and in the fuselage of airplanes. According to [2], thin plates are widely used in structures because they have excellent performance at imposed stresses, with the reduced weight of their elements, and, if added chrome, nickel or zinc to plates, high corrosion resistance. When a flat plate is subjected to transverse or axial loads, it develops stresses due to axial force, shear, bending, and torsion [3]. For [4] some factors must be analyzed with extreme care in the design of naval and offshore structures. The idealization and the design of a structural element should satisfy specific requirements of resistance, rigidity, and stability. In its great majority, structures as the ship hulls are formed basically by the association of beams, columns and plates, which are usually submitted to compression loads. In this context, when a slender structural element is subjected to compressive strengths, an extremely important phenomenon called buckling may occur, that is, making the element susceptible to instability.

Moreover, the designers should observe carefully the presence of perforations in plates. These can be used with the objective of decrease the total weight of the structure or to make possible the people's access to certain sections or services, or still, as elements with an aesthetic purpose. However, the inclusion of perforations in the plates causes a redistribution of their stresses, and may even lead to modifications in their mechanical strength and in the buckling characteristics [5]. Other aspects related to perforations, such as the geometry, the dimension and the positioning of the perforation, influence directly in the performance of a plate submitted to uniaxial compression [6].

Several researchers have studied the mechanical behavior of thin steel plates subjected to compression, and among them can be cited: [7] determined the values of critical buckling loads in rectangular plates with centralized perforations and subjected to biaxial loading using FEM; [8] have developed, validated and summarized analytical expressions whose purpose is to estimate the influence of single or multiple perforations in determining the value of the critical buckling load of plates in bending or compression; [9] applied the Constructal Design method for the optimization of perforated thin steel plates submitted to the elastic buckling; [10] used the Constructal Design method to evaluate the influence of the type and the shape of centralized perforations in thin steel plates subjected to linear elastic and nonlinear elasto-plastic buckling; and [11] studied the mechanical behavior to nonlinear buckling of thin rectangular steel plates with rectangular perforations and rounded vertices subjected to uniform compression.

Although there exists a significant number of scientific works addressed to the study of the elastic buckling in plates, there is a reduced number of these referring to the elasto-plastic buckling. This paper proposes to analyze the mechanical behavior of perforated thin steel plates subjected to uniaxial compression, using the computational modeling allied to the Constructal Design method for the generation of limit curves for elasto-plastic buckling. In this context, the type, the shape and the size of the perforation are essential parameters to be analyzed.

In order to aid in understanding the next sections of this article, a list of abbreviations a and a list of symbols are presented in the Appendix.

2. Buckling and Post-Buckling of Plates

As already mentioned, according to [4], the majority of the parts that integrate a naval structure are composed of plates, beams and columns, which are, in several situations, subjected to compressive loads. Structural components as plates, for instance, when submitted to compression or tension forces, possess differentiated behavior. Plates axially

tensioned develop shear stresses, on the other hand, when submitted to compressive strengths it can occur its transverse deflection, which is called buckling. Therefore, it is extremely important considering the buckling phenomenon in the procedures that involve the structural design of naval and offshore structures. Evidently, this procedure should be used for any structural component that is under the influence of the buckling phenomenon.

When a thin plate subjected to compression reaches its critical load value P_{cr}, the plate undergoes a sudden transverse deformation and may lose its ability to withstand loading, which would result in the collapse of the structure. The transverse deformation is curvilinear and graphically shows the buckling phenomenon. Moreover, according to [12], the application of a compression load, but less than the critical load value, does not cause the buckling phenomenon. In this case, a small perturbation (small lateral load or small initial curvature) causes a curvilinear deformation (lateral displacement) in the plate, but with the retreat of this, the plate returns to its initial configuration. However, for the least increase of the load beyond the critical value, a great transverse displacement occurs in the structure, that can cause the collapse of the plate.

According to [13], the analytical solution to the problem of elastic buckling in thin steel plates without perforation subjected to uniaxial compression is:

$$P_{cr} = k\frac{\pi^2 D}{H^2} \tag{1}$$

where, P_{cr} is the critical load per unit of length, π is a mathematical constant, D is the plate bending stiffness, and k is a function of the aspect ratio H/L. The plate bending stiffness and the buckling coefficient are defined, respectively, by:

$$D = \frac{Eh^3}{12(1-\nu^2)} \tag{2}$$

$$k = \left(m\frac{H}{L} + \frac{1}{m}\frac{L}{H}\right)^2 \tag{3}$$

being, E and ν, respectively, the modulus of elasticity and the Poisson's ratio of the plate's material, h the plate thickness, and m the number of half-waves of the deformation pattern in the x-axis direction.

A thin plate does not enter in collapse soon after the occurrence of the elastic buckling, but actually it can support loads significantly larger than the critical load without deforming excessively. The behavior of plates differs from that expected when considering the behavior of elastic bars submitted to compression that only withstands a slight increase in the load before excessive deformation of the bar occurs (see Fig. 1). The additional post-buckling resistance of thin plates is due to several factors however, the main one is that the deformed shape of the buckling plate cannot be developed from the pre-buckling configuration without a redistribution of the stresses in the mid-plane along the plate. This redistribution, which is ignored in the theory of small displacements of elastic buckling, usually favors the less rigid regions of the plate and causes an increase in plate efficiency. One of the most common causes of this redistribution is associated with the boundary conditions in the plane of the loaded edges of the plate [14].

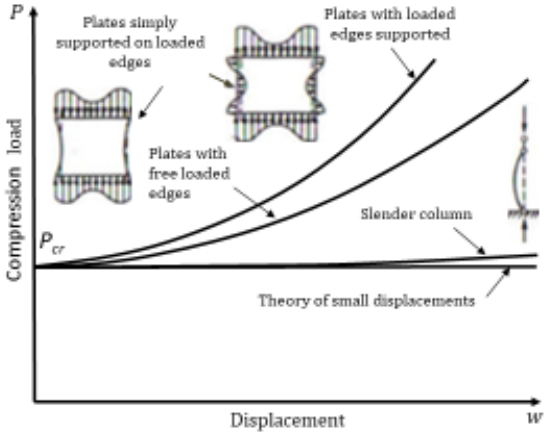

Fig. 1 Post-buckling behavior in slender plates, adapted of [15]

The load that defines the collapse of a plate, in its elasto-plastic behavior, is called post-critical or ultimate load, being represented by P_u. However, as already mentioned, the final load capacity of a plate is not restricted to the occurrence of elastic buckling, i.e., the plates resist load higher than the critical load, which allows an increase of load after the occurrence of elastic buckling [12]. Still in agreement with [12], the capacity of the plates support this load increment is associated with the formation of a membrane force that stabilizes the displacement through a transverse tension (see Fig. 2). When the external load is increased in order to cause the plate buckling, it occurs a non-uniform distribution of the stresses caused by the external load. This provides an increased resistance, which is due to the fact that the transverse fibers are tensioned after the buckling, tending to stabilize the longitudinal fibers.

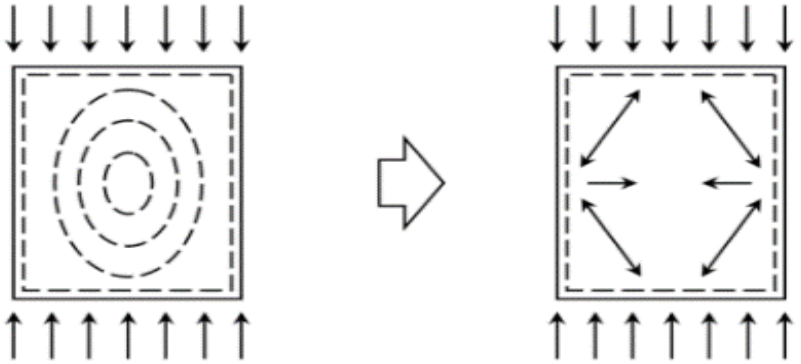

Fig. 2 Redistribution of stresses in the post-buckling critical state [12]

As described above, unlike the behavior of bars, plates exhibit significant resistance after the occurrence of buckling. In addition, if this post-critical resistance is fully utilized, a structural, efficient and economic design may be obtained [16]. According to [17] the post-critical loading reserve is not unlimited, and according to experimental results, the plate reaches the collapse when the maximum compressive stress at the edges not charged reach the elastic limit. Still according to [17], Bleich proposed in 1924 the Eq. 4 to calculate

buckling of plates in the elasto-plastic regime, where $\tau = E_t/E$, and E_t corresponds to the steel tangent modulus of elasticity.

$$\frac{\partial^4 w}{\partial x^4} + 2\sqrt{\tau}\frac{\partial^4 w}{\partial x^2 \partial y^2} + \frac{\partial^4 w}{\partial y^4} + \frac{\sigma_x h}{D}\frac{\partial^2 w}{\partial x^2} = 0 \quad (4)$$

In Eq. 4, the term $\sqrt{\tau}$ is the plastic reduction factor of a plate subjected to uniform compression stress in one direction, being this factor variable with the type of loading and with the boundary conditions of the plate. According to [17], the analysis of the differential equation proposed by von Karman, 1910, and after by Bleich, 1924, to elasto-plastic analysis is quite complex, being normally necessary resort to numerical and computational methods.

3. Constructal Design Method

The Constructal Theory stands out for present time context and for the perception of the design importance of natural structures. As a basic reference, it is based on the perception that the design of natural structures is directly related to the occurrence of a physical phenomenon, which occurs in small and large systems such as rivers, traffic in cities, vascularized living tissue, the dissemination of ideas, among others. Its guidelines and its major advances in science are directly related to the studies developed by its founder, Adrian Bejan, and researchers who use it in different areas of knowledge. The line of reasoning where forms from nature are accepted, observed, and copied are still present today. However, the Constructal Theory, according to [18], proposes the inversion of this thought, that is, initially invokes the Constructal law and with that, theoretically, the architecture of the form is deduced. Then, the theoretical configuration obtained in the deduction is compared with that of the natural phenomena, and the agreement between the geometries is what validates the Constructal Law.

According to [19], the Constructal Law for flow generation and configuration is defined as: "For a finite-size flow system to persist in time (to live), its configuration must evolve in such a way that provides greater and greater access to the currents that flow through it". This law corresponds to the basis of the Constructal Theory and represents a new extension of thermodynamics: the thermodynamics of systems out of balance and with constraints. Some confuse the Constructal Law with an assumed natural evolutionary trend with toward “more flow,” which is not correct. The natural tendency is to evolve freely into flow configurations that offer greater access to what flows, not more flow [20]. According to [21], in summary, the evolution of systems is strictly connected with the possibility of their morphing configuration, permitting that the new configurations replace existing configurations, to perform better (Constructal Law). This self-standing law of design has both local and global significance. It shows a fascinating connection between the Nature as a whole and what this law holds in our world. The paths of all natural flow systems (i.e., animate and inanimate systems) are drawn together and can be described and understood under a unified view. The application of the Constructal Law according to [18] occurs through the Constructal Method, called Constructal Design, and serves to predict many phenomena in nature and designs in engineering. This method is used to obtain configurations that optimize the flow systems through the optimal distribution of imperfections.

3.1 Constructal Design Application

The application of the Constructal Design method allows an adequate evaluation of the influence of the geometric configuration on the mechanical performance of a physical system. Taking into account that all the geometries proposed by the Constructal Design

method are evaluated, it can be said that there is a geometric optimization procedure through an exhaustive search process. Thus, in order to apply the Constructal Design method, it is fundamental to define some parameters, such as objective functions, degrees of freedom and constraints. After the definition of these parameters, it is possible to generate infinite geometries, enabling the application the exhaustive search method. However, according to [22] and [23], if the degrees of freedom and/or parameters are many, another optimization method can be used.

Here, the objective function seeks to maximize the ultimate stresses by varying the degrees of freedom H/L and H_0/L_0. The degrees of freedom relate, respectively, the width H to the length L of the plate and the width H_0 to the length L_0 of the perforation. For H/L, two possibilities were adopted: H/L = 1.0 and H/L = 0.5, while for H_0/L_0 several possible values were considered (being related to the perforation type and the problem constraints). The variables H, L, H_0 and L_0 as well as the perforation types used in this work are presented in Fig. 3. It is worth to mention that the plate without perforation, used to verify the computational model, is presented in Fig. 3a. Besides, values of H = 1000.00 mm and L = 2000.00 mm were considered for the plates with H/L = 0.5 and $H = L$ = 1414.21 mm for the plates with H/L = 1.0.

It was adopted, with the purpose of adequately comparing the different types of perforation and as a restriction to the resolution of the buckling problem, a fraction (Φ) for the perforation volume. This volume fraction is a function of the characteristic dimensions of each perforation type, being defined, respectively, for longitudinal oblong, transverse oblong, elliptical, rectangular, diamond, longitudinal hexagonal and transverse hexagonal cut out, as:

$$\Phi = \frac{V_0}{V} = \frac{\left((L_0 - H_0)H_0 + \frac{\pi}{4}H_0^2\right)h}{HLh} = \frac{(L_0 - H_0)H_0 + \frac{\pi}{4}H_0^2}{HL} \tag{5}$$

$$\Phi = \frac{V_0}{V} = \frac{\left((H_0 - L_0)L_0 + \frac{\pi}{4}L_0^2\right)h}{HLh} = \frac{(H_0 - L_0)L_0 + \frac{\pi}{4}H_0^2}{HL} \tag{6}$$

$$\Phi = \frac{V_0}{V} = \frac{(\pi H_0 L_0 h)/4}{HLh} = \frac{\pi H_0 L_0}{4HL} \tag{7}$$

$$\Phi = \frac{V_0}{V} = \frac{H_0 L_0 h}{HLh} = \frac{H_0 L_0}{HL} \tag{8}$$

$$\Phi = \frac{V_0}{V} = \frac{(H_0 L_0 h)/2}{HLh} = \frac{H_0 L_0}{2HL} \tag{9}$$

$$\Phi = \frac{V_0}{V} = \frac{H_0(L_1 + L_2)h}{HLh} = \frac{H_0(L_1 + L_2)}{HL} \tag{10}$$

$$\Phi = \frac{V_0}{V} = \frac{L_0(H_1 + H_2)h}{HLh} = \frac{L_0(H_1 + H_2)}{HL} \tag{11}$$

where, V_0 represent the perforation volume, V the total volume of the plate without perforation and h the plate's thickness.

For all studied cases in this work, plates with the total area without perforation of 2.00 m^2 and thickness of 10.00 mm were considered. In addition, as a geometric constraint, the

minimal distance between de cut out edge and the plate edge is H-H_0 = 200.00 mm and L-L_0 = 200.00 mm, respectively, in transverse and longitudinal directions (see Figs. 3b to 3h).

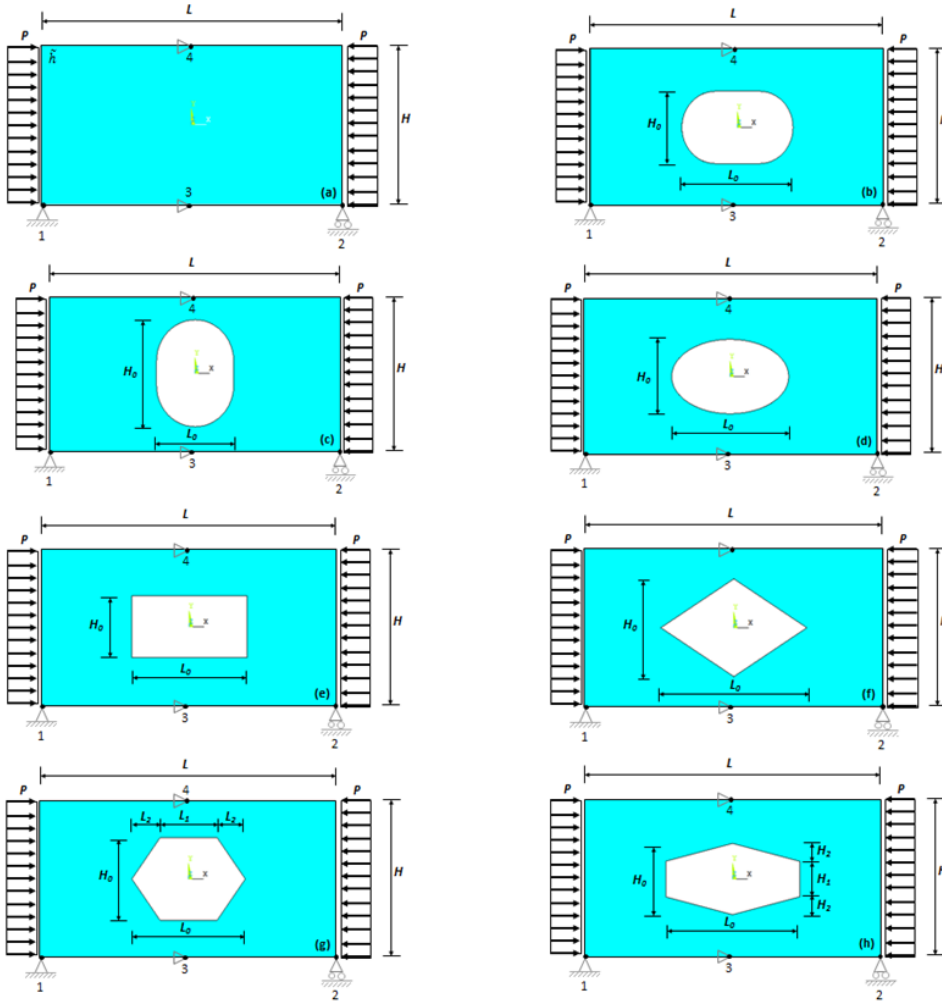

Fig. 3 Plate with: (a) no perforation, (b) longitudinal oblong perforation, (c) transverse oblong perforation, (d) elliptical perforation, (e) rectangular perforation, (f) diamond perforation, (g) longitudinal hexagonal perforation, and (h) transverse hexagonal perforation

5. Computational Models

The computational model used in this work to solve the problem of elasto-plastic buckling of thin steel perforated plates was developed in Ansys® software. For all numerical simulations, the SHELL93 finite element was adopted (see Fig. 4). This element, that can be used for the modeling of plates and shells, has eight nodes with six degrees of freedom in each node, being 3 translations and 3 rotations in the x, y, and z directions. The interpolating polynomials responsible for the deformation form are quadratic in both plane directions and the finite element in question can incorporate plasticity, hardening, and large deformations [24].

An example of discretization and mesh generation for the computational domain, using the SHELL93 finite element, is presented in Fig. 5. In this figure, the compression load *P*, the length *L*, the width *H* and the constraints are indicated. The plate has a constant thickness *h* of 10.00 mm. Concerning the boundary conditions, it was considered that the plates have all edges simply supported, i.e., all nodes along the four edges are restricted to deflection in *z* direction. Besides, the displacement in *x* direction is restricted at nodes 1, 3 and 4 as well as the displacement in *y* direction is restricted at nodes 1 and 2.

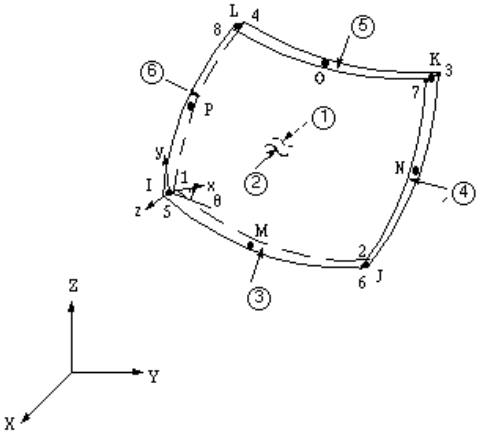

Fig. 4 SHELL93 element [24]

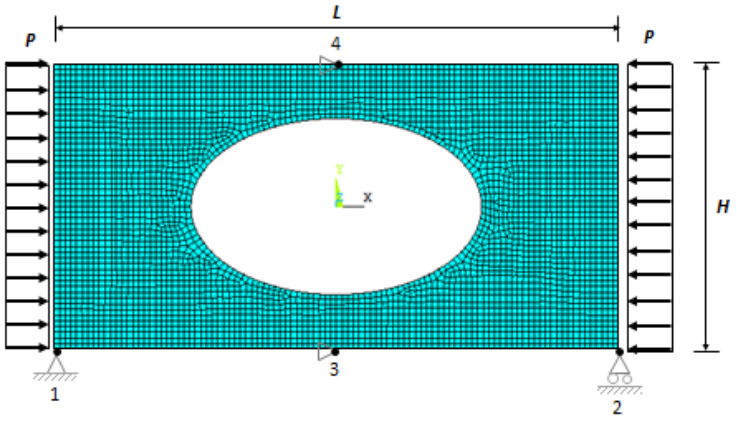

Fig. 5 Reference model generated in ANSYS®

5.1 Elastic and Elasto-plastic Plate Buckling

The numerical procedure used to calculate the load that causes elastic buckling is based on an analysis of eigenvalues and eigenvectors. Once assumed that the structure presents a linear elastic behavior, a structural instability is foreseen, being the focus of the study the verification of the load that provokes the elastic buckling of the plate. For this analysis type, that involves the equilibrium conditions of the finite element equations, it is necessary the solution of homogeneous algebraic equations, where the smallest eigenvalue and eigenvector correspond, respectively, to the critical buckling load and the elastic deformation mode of the structure [25].

This consideration is necessary because the exact post-buckling problem does not allow for a direct analysis due to problems of response discontinuities at the bifurcation point. Starting from the first elastic buckling mode configuration, [26] defines that the maximum value to be assumed for the initial imperfection should obey the relationship $H/2000$, where H represents the width of the plate. Then, the ultimate load on the plate can be found using as reference the load $P_y = \sigma_y t$, where σ_y represents the material yielding strength. This load should be applied in small loading increments on the plate in the direction parallel to the x-axis. As already adopted in [27], for each load increment the Newton-Raphson method is used to determine the displacements corresponding to the equilibrium configuration of the plate through the equations:

$$\{P\}_{i+1} = \{P\}_i + \{\Delta P\} \tag{12}$$

$$\{\psi\} = \{P\}_{i+1} - \{F_{NL}\} \tag{13}$$

$$[K_t]\{\Delta U\} = \{\psi\} \tag{14}$$

$$\{U\}_{i+1} = \{U\}_i + \{\Delta U\} \tag{15}$$

where $[K_t]$ is the updated tangent stiffness matrix, $\{\Delta U\}$ corresponds to the vector of incremental displacements required to achieve the equilibrium configuration, $\{F_{NL}\}$ represents the vector of internal nonlinear nodal forces and $\{\psi\}$ is the vector of unbalanced forces. The vectors $\{U\}_i$ and $\{U\}_{i+1}$ correspond to the displacements, while the vectors $\{P\}_i$ and $\{P\}_{i+1}$ correspond to the external loads applied, to two successive equilibrium configurations of the structure, respectively.

If at a certain load level the convergence can not be reached, or in other words, a finite displacement increment can not be defined so that the unbalanced forces vector $\{\psi\}$ is nullified, this means that the structure failure load has been achieved. This occurs because no matter as large as the displacements and strains can be, the stresses and internal forces can not enhance as it would be necessary to balance the external loads. Therefore, in this case, the maximum resistance capacity of the material was reached [27].

The external compression load on the plate, used in this work for the elasto-plastic buckling analysis, was divided into 100 load increments with a maximum of 200 iterations for each load increment.

6. Results and Discussion

Initially, the results will be presented for the verification of the computational model for the linear elastic buckling analysis and validation of the computational model for the nonlinear elasto-plastic buckling analysis. Then, the thin steel plates with H/L = 1.0 and H/L = 0.5, with various central perforation types (elliptical, rectangular, diamond, longitudinal hexagonal, transversal hexagonal, longitudinal oblong and transversal oblong), with different sizes (Φ = 0.08, 0.10, 0.15, 0.20 and 0.25) and for different geometric forms (obtained by the H_0/L_0 variation) are subjected to elasto-plastic buckling.

6.1 Verification and Validation

The computational model verification for the analysis of elastic buckling was performed by comparing the result of the critical load of a thin plate of steel without perforation with the analytical solution given by Eq. 1. It was considered a simply supported plate in its four

edges, with the following mechanical and dimensional properties: E = 210 GPa, ν = 0.30, σ_y = 250 MPa, H = 1000.00 mm, L = 2000.00 mm and h = 10.00 mm. It was used a structured and converged mesh, generated with the assistance of a finite square element of side 20.00 mm, obtaining a critical stress of σ_{cr} = 75.37 MPa. This value, when compared to the analytical result (σ_{cr} = 75.92 MPa), represents a difference of -0.72%, verifying the developed computational model.

After that, the computational model validation for the analysis of elasto-plastic buckling was performed considering the value of the ultimate load experimentally obtained in [26] for the comparison. For this purpose, a thin steel plate was used, simply supported in the four borders, with the dimensions H = L = 1000.00 mm and h = 20.00 mm, and with the mechanical properties: E = 210 GPa, ν = 0.30, σ_y = 350 MPa, with centralized circular perforation with diameter of 300.00 mm. The computational domain was discretized using a finite element with the maximum size of 20.00 mm. The ultimate stress determined experimentally in [26] was of σ_u = 213.50 MPa, and the result obtained by numerical simulation in this work was of σ_u = 217.00 MPa, which represents a difference of 1.64%, validating the proposed computational model.

6.2 Normalization of the Limit Stress

Here the objective is to define the limit curve that prevents the occurrence of elasto-plastic buckling. To do so, it is necessary to normalize the ultimate stresses, by means the equation:

$$NLS_{EP} = \frac{\sigma_u}{\sigma_y} \tag{16}$$

where NLS represents the normalized limit stress and the subscript EP refers to elasto-plastic buckling. For all studied cases, the following properties of the material were considered: E = 210 GPa, ν = 0.30, σ_y = 250 MPa and h = 10.00 mm, respectively, for modulus of elasticity, Poisson's ratio, material yielding strength and thickness of the plate.

The H_0/L_0 variation, i.e. the perforation shape variation, allows the generation of an elasto-plastic buckling limit curve for each perforation size and for each perforation type. To exemplify, the plates with H/L = 1.0 and H/L = 0.5, for Φ = 0.20, having an elliptical perforation were considered, being its limit curves showed in Figs. 6a and 6b, respectively. The NLS_{Max} and NLS_{Min} factors are indicated in Fig. 6, corresponding to maximum and minimum normalized limit stresses and identify, respectively, the optimal geometry and the worst geometry. Regarding the normalized stresses, it was found that, in several situations and for several values of H_0/L_0, the stresses acting on the plates exceeded the limit to elastic buckling.

So to take into account all studied perforation types the following nomenclature was employed: elliptic (E), rectangular (R), diamond (D), longitudinal hexagonal (LH), transverse hexagonal (TH), longitudinal oblong (LO), and transverse oblong (TO). Therefore, Figs. 7 to 11 show the elasto-plastic buckling limit curve for the plates with H/L = 1.0 and H/L = 0.5, for all volume fractions Φ and all type of perforations.

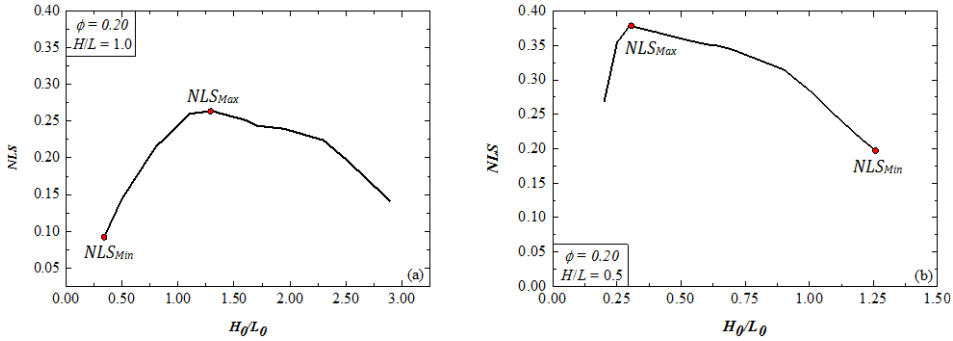

Fig. 6 Limit curve for the occurrence of elasto-plastic buckling in plates with elliptical perforation, for Φ = 0.20: (a) H/L = 1.0 e (b) H/L = 0.5

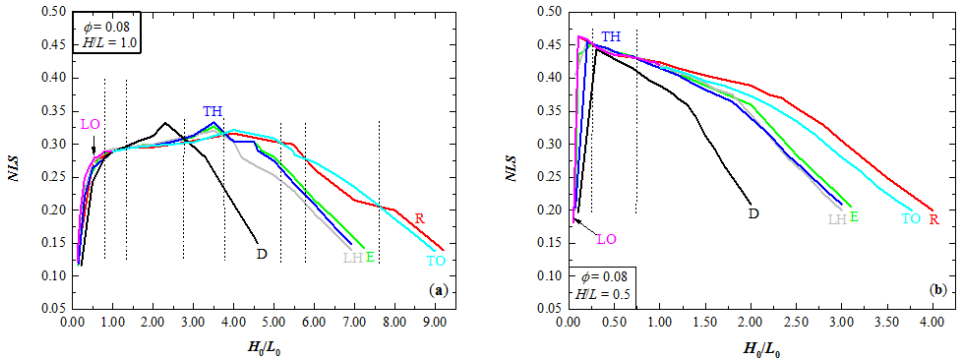

Fig. 7 Limit curves for the occurrence of the elasto-plastic buckling for all types of perforation, and for Φ = 0.08: (a) H/L = 1.0 e (b) H/L = 0.5

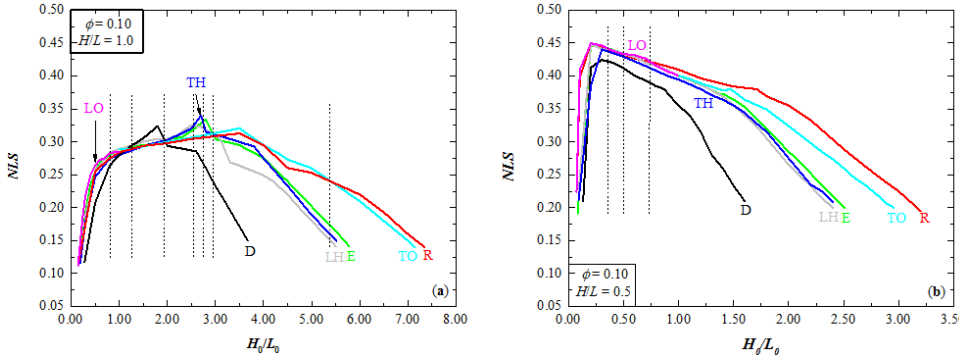

Fig. 8 Limit curves for the occurrence of the elasto-plastic buckling for all types of perforation, and for Φ = 0.10: (a) H/L = 1.0 e (b) H/L = 0.5

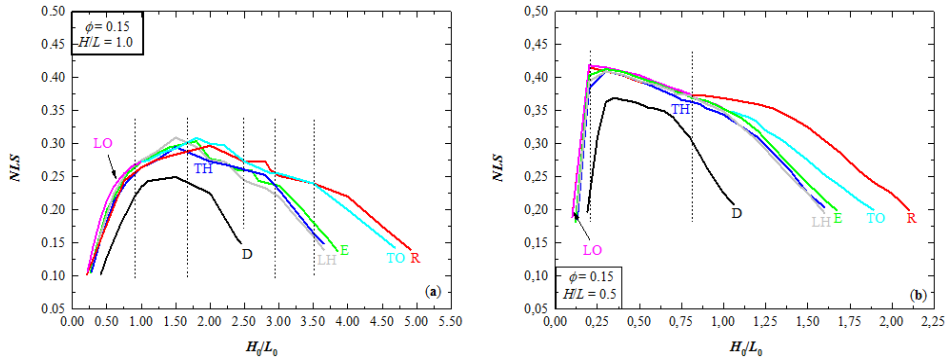

Fig. 9 Limit curves for the occurrence of the buckling for all types of perforation, and for Φ = 0.15: (a) H/L = 1.0 e (b) H/L = 0.5

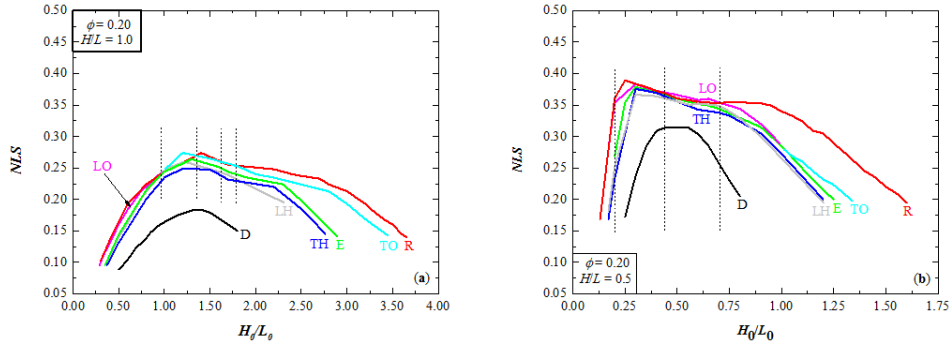

Fig. 10 Limit curves for the occurrence of the elasto-plastic buckling for all types of perforation, and for Φ = 0.20: (a) H/L = 1.0 e (b) H/L = 0.5

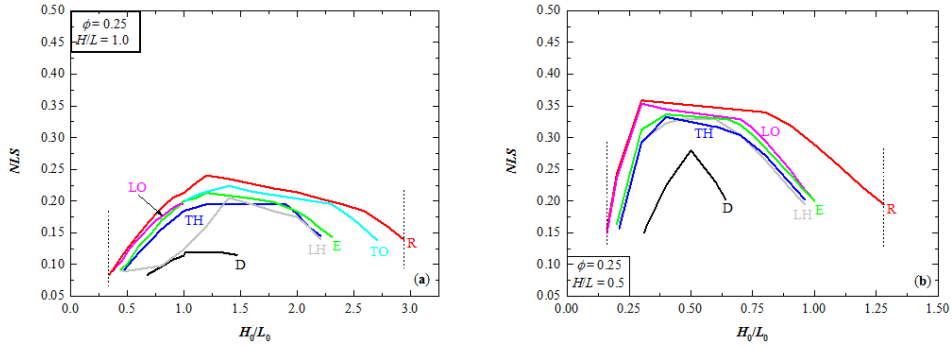

Fig.11 Limit curves for the occurrence of the elasto-plastic for all types of perforation, and for Φ = 0.25: (a) H/L = 1.0 e (b) H/L = 0.5

The Figs. 7-11 show some recurrent aspects for the mechanical behavior of the limit curves considering the elasto-plastic buckling. Among them, in a general w, it is possible to highlight that: first, the plates with rectangular perforation present the greatest range for the variation of H_0/L_0, and those with to diamond perforation, the least range; second, there is a graphical similarity in the representation of the limit curves for Φ = 0.08 and 0.10

and for Φ = 0.15, 0.20 and 0.25; third, the plates with transverse hexagonal, longitudinal hexagonal and elliptical perforation type, present values very close to H_0/L_0; fourth, the values of maximum stresses to the plates with H/L = 1.0, defined from the NLS_{EP}, are found for higher values of degree of freedom H_0/L_0 when compared to the plates H/L = 0.5; fifth, the plates with H/L = 0.5 show higher loading capacity compared to the plates with H/L = 1.0; sixth, there is no universal perforation type that conducts to the best mechanical performance regarding the degree of freedom H_0/L_0, instead there are intervals in which one perforation type has better results than the other types, e.g. in plates with H/L = 0.5 and for Φ = 0.20, in the interval $0.44 < H_0/L_0 \leq 0.70$, the best perforation type is the rectangular, and; finally, the geometric shape of the perforation, i.e., the variation of its geometric configuration on the *x* and *y*-axes, is important for the development of the elasto-plastic buckling limit curves, causing an increase or decrease in the mechanical performance of the plates.

In order to quantify the improvement in the mechanical behavior of the plates, Table 1 shows the results obtained comparing the best and the worst geometries for each specific type of perforation and for each value of Φ.

According to Table 1, the best mechanical performance for the plates with H/L = 1.0 corresponds to an increase of 191.85% for the plates with Φ = 0.10 and transverse hexagonal perforation, while for the plates with H/L = 0.5 an improvement of 154.03% was achieved for the longitudinal oblong perforation type and Φ = 0.08. In turn, the worst mechanical performance, of 42.82%, refers to the plates with H/L = 1.0, was obtained with Φ = 0.25 and diamond perforation, as well as, of 36.54% for plates with H/L = 0.5, reached with Φ = 0.20 and longitudinal oblong perforation.

Considering the mechanical performance for each studied perforation volume fraction Φ, it was observed:

Plates with Φ = 0.08 for H/L = 1.0 and for H/L = 0.5 reached improvements of 185.41% for diamond perforation and 155.71% for rectangular perforation, respectively; while the worst obtained results were 132.97% and 107.50%, respectively, both for transversal oblong perforation.

Plates with Φ = 0.08 for H/L = 1.0 and for H/L = 0.5 achieved improvements of 191.85% for transversal hexagonal perforation and 134.26% for elliptical perforation, respectively; while the worst results correspond, respectively, to 132.14% and 100.00% for plates with transversal oblong perforation.

Plates with Φ = 0.15 for H/L = 1.0 and H/L = 0.5 presented improvements of 189.85% for rectangular perforation and 126.30% for elliptical perforation, respectively; and the worst results were 116.08% and 74.50%, respectively, for plates with transversal oblong perforation.

Plates with Φ = 0.20 for H/L = 1.0 and H/L = 0.5 showed improvements of 176.44% for elliptical perforation and 130.88% for rectangular perforation, respectively; whereas the worst behaviors were 92.28% for transversal oblong perforation and 36.56% for rectangular perforation, respectively.

Plates with Φ = 0.20 for H/L = 1.0 and H/L = 0.5 achieved improvements of 176.44% for elliptical perforation and of 130.88% for rectangular perforation, respectively; being the worst results of 92.28% for transversal oblong perforation and of 36.56% for longitudinal oblong perforation, respectively.

Plates with Φ = 0.25 for H/L = 1.0 and H/L = 0.5 reached improvements of 186.31% for rectangular perforation and 137.25% for longitudinal oblong perforation, respectively;

whilst the worst results were of 42.86% and 86.67%, respectively, both for diamond perforation.

The application of the Constructal Design method allows an adequate comparison about the von Mises stress distribution among the studied plates. Thus, to illustrate how the principle of optimal distribution of imperfections actually leads to superior performances, the Figs. 12 and 13 show the distribution of von Mises stresses for the best and worst geometries, according to the data exposed in the Table 1, for H/L = 1.0 with Φ = 0.10 and for H/L = 0.5 with Φ = 0.20, respectively.

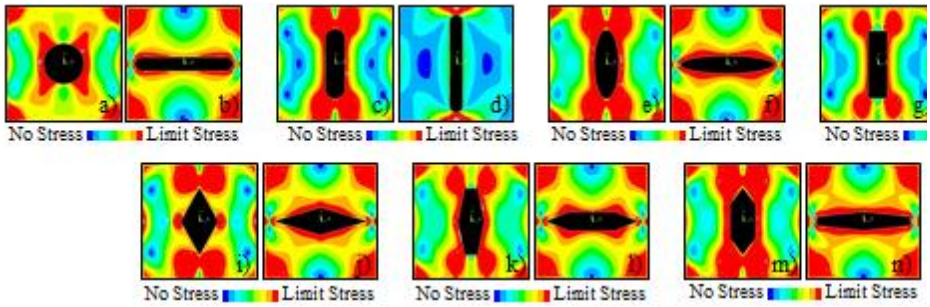

Fig. 12 Distribution of the von Mises stress in plates with H/L = 1.0, for all perforation types, and Φ = 0.10, being: (a, c, e, g, i, k, m), the best; and (b, d, f, h, j, l, n), the worst configurations

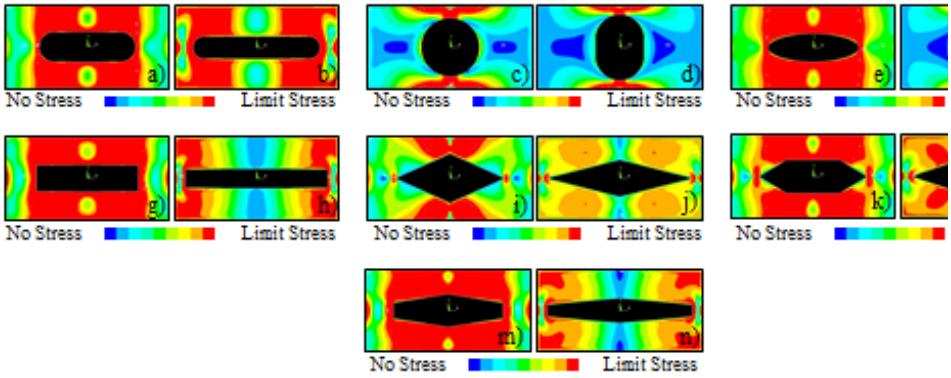

Fig. 13 Distribution of the von Mises stress in plates with H/L = 0.5, for all perforation types, and Φ = 0.20, being: (a, c, e, g, i, k, m), the best; and (b, d, f, h, j, l, n), the worst configurations

The Figs. 12 and 13 show that the plates with the optimized geometries have the best distribution of the material yielding stress at failure when compared with the plates with the worst geometries. Visually, this means that the optimal geometries have a larger region subjected to the limit stress (which is represented by the red color). In this context, the improvement in mechanical performance obtained in the optimized geometries is in accordance with the principles defined by the Constructal Theory, that is, this geometry promotes the better distribution of the imperfections [18].

Table 1: Best and worst geometries for all cases studied

	Hole type	H/L = 1.0					H/L = 0.5				
		$\left(\frac{H_0}{L_0}\right)_o$	NLS_{Max}	$\frac{H_0}{L_0}$	NLS_{Min}	Diff. %	$\left(\frac{H_0}{L_0}\right)_o$	NLS_{Max}	$\frac{H_0}{L_0}$	NLS_{Min}	Diff. %
ϕ = 0.08	LO	0.99	0.2890	0.12	0.1227	135.53	0.10	0.4636	0.05	0.1825	154.03
	TO	4.00	0.3215	8.99	0.1380	132.97	1.01	0.4150	3.77	0.2000	107.50
	E	3.50	0.3271	0.14	0.1165	180.77	0.25	0.4515	3.10	0.2050	120.24
	R	4.00	0.3165	0.12	0.1253	152.59	0.10	0.4636	0.05	0.1813	155.71
	D	2.30	0.3325	0.22	0.1165	185.41	0.30	0.4440	0.10	0.1972	125.15
	LH	3.50	0.3205	0.15	0.1227	161.21	0.20	0.4581	3.00	0.2000	129.05
	TH	3.50	0.3330	0.15	0.1190	179.83	0.20	0.4555	0.07	0.2036	123.72
ϕ = 0.10	LO	0.99	0.2840	0.14	0.1115	154.71	0.20	0.4496	0.07	0.2236	101.07
	TO	3.50	0.3250	7.15	0.1400	132.14	1.01	0.4000	2.96	0.2000	100.00
	E	2.80	0.3340	0.18	0.1178	183.53	0.20	0.4465	0.08	0.1906	134.26
	R	3.50	0.3130	0.14	0.1115	180.72	0.20	0.4495	3.20	0.1950	130.51
	D	1.80	0.3240	0.28	0.1177	175.28	0.30	0.4245	1.60	0.2096	102.53
	LH	2.50	0.3255	0.19	0.1203	170.57	0.20	0.4476	2.40	0.2000	123.80
	TH	2.70	0.3400	0.19	0.1165	191.85	0.30	0.4405	2.40	0.2090	110.77
ϕ = 0.15	LO	0.99	0.2730	0.22	0.1075	153.95	0.20	0.4186	0.10	0.1889	121.60
	TO	1.80	0.3090	4.68	0.1430	116.08	1.05	0.3490	1.89	0.2000	74.50
	E	1.80	0.3040	0.26	0.1050	189.52	0.30	0.4130	0.12	0.1825	126.30
	R	2.00	0.2971	0.21	0.1025	189.85	0.20	0.4155	0.10	0.1906	118.00
	D	1.50	0.2500	0.41	0.1025	143.90	0.35	0.3695	0.19	0.1972	87.37
	LH	1.50	0.3095	0.28	0.1075	187.91	0.20	0.4096	1.60	0.1986	106.24
	TH	1.50	0.2950	0.28	0.1075	174.42	0.30	0.4096	0.13	0.1863	119.86
ϕ = 0.20	LO	0.99	0.2440	0.29	0.0950	156.84	0.30	0.3830	0.17	0.2805	36.54
	TO	1.60	0.2740	3.45	0.1425	92.28	1.01	0.2800	1.34	0.1980	41.41
	E	1.30	0.2640	0.35	0.0955	176.44	0.30	0.3786	1.25	0.2000	89.30
	R	1.40	0.2740	0.30	0.1025	167.32	0.25	0.3895	0.13	0.1687	130.88
	D	1.30	0.1840	0.55	0.0890	106.74	0.45	0.3150	0.25	0.1725	82.61
	LH	1.20	0.2600	0.37	0.1000	160.00	0.30	0.3665	0.17	0.1813	102.15
	TH	1.50	0.2490	0.37	0.0955	160.73	0.30	0.3756	0.17	0.1687	122.64
ϕ = 0.25	LO	0.99	0.1955	0.37	0.0890	119.66	0.30	0.3535	0.16	0.1490	137.25
	TO	1.20	0.2240	2.71	0.1380	62.32	-	-	-	-	-
	E	1.20	0.2130	0.44	0.0915	132.79	0.40	0.3365	0.20	0.1640	105.18
	R	1.20	0.2405	0.34	0.0840	186.31	0.30	0.3586	0.16	0.1555	130.61
	D	1.01	0.1200	0.68	0.0840	42.86	0.50	0.2800	0.31	0.1500	86.67
	LH	1.40	0.2050	0.46	0.0890	130.34	0.47	0.3300	0.21	0.1650	100.00
	TH	1.40	0.1950	0.46	0.0890	119.10	0.40	0.3326	0.21	0.1573	111.44

7. Conclusions

Computational models associated to the Constructal Design were used to analyze the influence of the geometric configuration of perforations on thin steel plates subjected to elasto-plastic buckling. It was possible, through these analyses, to obtain the values of the ultimate stresses in the elasto-plastic buckling. To do so, the type (longitudinal oblong, transverse oblong, elliptic, rectangular, diamond, longitudinal hexagonal, and transverse hexagonal), shape (by means the variation of H_0/L_0 ratio) and size (through of volume fraction Φ variation) of perforations were evaluated.

The H_0/L_0 variation allows the definition of elasto-plastic buckling limit curve for all studied type and size of perforations. These curves represent the collapse of the plates by yielding of the material and indicate the effect of shape perforation in each case, being this a scientific contribution of the present work.
The obtained results show a variation in the mechanical performance improvement from 42.86% to 191.85% for the plates with H/L = 1.0, and from 36.54% to 155.71% for the plates with H/L = 0.5.

According to the type of perforation, the best mechanical performances obtained for the plates with H/L = 1.0 were: 156.8% for longitudinal oblong perforation plates and Φ = 0.20; 132.9% for the plates with transversal oblong perforation and Φ = 0.08; 189.5% for plates with elliptical perforation and Φ = 0.15; 189.8% for plates with rectangular perforation and Φ = 0.15; 185.4% for plates with diamond perforation and Φ = 0.08; 187.9% for the plates with longitudinal hexagonal perforation and Φ = 0.15; 191.8% for the plates with transverse hexagonal perforation and Φ = 0.10. For the plates with H/L = 0.5, there were: 154.0% for the plates with longitudinal oblong perforation and Φ = 0.08; 107.5% for plates with transverse oblong perforation and Φ = 0.08; 134.2% for plates with elliptical perforation and Φ = 0.10; 155.7% for plates with rectangular perforation and Φ = 0.08; 125.1% for plates with diamond perforation and Φ = 0.08; 129.0% for the plates with longitudinal hexagonal perforation and Φ = 0.08; 123.7% for the plates with transverse hexagonal perforation and Φ = 0.08. Hence, the plates with H/L = 1.0 presented a higher mechanical performance than the plates with H/L = 0.5, considering all types of perforation, for Φ = 0.10, Φ = 0.15, and Φ = 0.20. The exceptions refer to plates with oblong longitudinal and rectangular perforations, for Φ = 0.08; and with oblong longitudinal and diamond perforation for Φ = 0.25.

Lastly, the use of the Constructal Design method associated with computational modeling allowed to show the importance that the geometric evaluation has for the definition of the mechanical behavior of the plates in elasto-plastic buckling. Its application made it possible to compare adequately the results obtained for all types and geometric forms of the proposed perforations. It was possible to evaluate the influence of the type, shape, and size of the perforation on the mechanical behavior of the plates as a function of H/L and H_0/L_0. In this sense, the Constructal Design method was used to define, through the analysis of the imperfection distribution, the optimal geometry for each H/L ratio, for each volume fraction (Φ) of the perforation, and for each type of perforation. It was verified that the optimal geometry, i.e., the geometry that promotes the maximization of the ultimate buckling stress, is in agreement with the statement: "The structures that present the best mechanical performance also present the best distribution of their imperfections, which is in accordance with the principles defined in the Constructal theory [18, 28].

8. Acknowledgments

The authors thank FAPERGS (Research Support Foundation of Rio Grande do Sul), CNPq (Brazilian National Council for Scientific and Technological Development) and CAPES Brazilian Coordination for Improvement of Higher Education Personnel) for the financial support.

Nomenclature

D	Diamond perforation	E_t	steel tangent modulus of elasticity
E	Elliptical perforation	H	plate width
EP	Elasto-Plastic buckling	h, t	plate thickness
FEM	Finite Element Method	H/L	relation between the width and the length of the plate
LH	Longitudinal Hexagonal perforation	H_0	perforation width
LO	Longitudinal Oblong perforation	H_0/L_0	relation between perforation width and length
NLS	Normalized Limit Stress	k	function of the aspect ratio
R	Rectangular perforation	L	plate length
TH	Transversal Hexagonal perforation	L_0	perforation length
TO	Transversal Oblong perforation	m	number of half-waves of the deformation pattern in the x-axis direction
$\left(\frac{H_0}{L_0}\right)_o$	best geometry	NLS_{Max}	maximum normalized limit stresses
$\{F_{NL}\}$	vector of internal nonlinear nodal forces	NLS_{min}	minimum normalized limit stress
$[K_t]$	updated tangent stiffness matrix	P_{cr}	critical load per unit of length
$\{P\}_i$	external load applied	P_u	ultimate load per unit of lenght
$\{P\}_{i+1}$	external load applied	V	total volume of the plate without perforation
$\{U\}_i$	displacement	V_0	perforation volume
$\{U\}_{i+1}$	displacement	ν	poisson's ratio of the plate's material
$\{\Delta U\}$	vector of incremental displacements	π	mathematical constant
$\sqrt{\tau}$	plastic reduction factor of a plate subjected to uniform compression stress in one direction	σ_{cr}	critical stress
$\{\psi\}$	vector of unbalanced forces	σ_u	ultimate stress
D	plate bending stiffness	σ_y	material yielding strength
E	modulus of elasticity	Φ	fraction for the perforation volume

References

[1] Bellei IH. Edifícios Industriais em Aço: Projeto e Cálculo, Pini, São Paulo, SP, Brazil, 2006.
[2] Silva VP. Design of Steel Structures, Course notes - USP, São Paulo, SP, Brazil, 2012.

[3] Ventsel E, Krauthammer T. Thin Plates and Shells, Marcelo Dekker, New York, NY, USA, 2001.
[4] Okumoto Y, Takeda Y, Mano M, Okada T. Design of Ship Hull Strucutures: A practical Guide for Engineers, Springer,Yokohama, Japan, 2009. https://doi.org/10.1007/978-3-540-88445-3
[5] Cheng B, Zhao JS. Strengthening of perforated plates under uniaxial compression: Buckling analysis. Thin-Walled Structures, 2010; 48(12): 905-914. https://doi.org/10.1016/j.tws.2010.06.001
[6] Chow F, Narayanan R. Buckling of Plates Containing Openings, Seventh International Specialty Conference on Cold-Formed Steel Structures, 1984
[7] El-Sawy KM, Martini MI. Elastic stability of bi-axially loaded rectangular plates with a single circular hole, Thin-Walled Structures, 2007; 45(1): 122-133. https://doi.org/10.1016/j.tws.2006.11.002
[8] Moen CD, Schafer BW. Elastic buckling of thin plates with holes in compression or bending, Thin-Walled Structures, 2009; 47(12): 1597-1607. https://doi.org/10.1016/j.tws.2009.05.001
[9] Helbig D, Real MV, Correia ALG, Dos Santos ED, Rocha LAO., Isoldi LA. Constructal Design of perforated steel plates subject to linear elastic and nonlinear elasto-plastic buckling. XXXIV Iberian Latin American Congress on Computational Methods in Engineering, 2013.
[10] Lorenzini G, Helbig D, Da Silva CCC, Real MV, Dos Santos ED, Isoldi LA. Constructal design method applied to the analysis of the cutout type and cutout shape influences in the mechanical behavior of thin steel plates subjected to buckling, Constructal Law & Second Law Conference, 2015
[11] Falkowicz K, Ferdynus M, Debski H. Numerical analysis of compressed plates with a cut-out operating in the geometrically nonlinear range, Science and Technology, 2015; 17(2): 222-227. https://doi.org/10.17531/ein.2015.2.8
[12] Åkesson B. Plate Buckling in Bridges and other Structures, Taylor & Francis Group, London, England, 2007.
[13] Vinson JR. Plate and Panel Structures of Isotropic, Composite and Piezoelectric Materials, Including Sandwich Construction, Springer Science & Business Media, 2005. https://doi.org/10.1007/1-4020-3111-4
[14] Chajes A. Principles of Structural Theory, Prentice-Hall, Englewood Cliffs, NJ, USA, 1974.
[15] Bradford MA, Cuk PE. Elastic buckling of tapered monosymmetric I-beams, Journal of Structural Engineering, 1988; 114(5); 977-996. https://doi.org/10.1061/(ASCE)0733-9445(1988)114:5(977)
[16] Mulligan GP, Peköz T. The influence of local buckling on the structural behavior of single-symmetric cold-formed steel columns, Center for Cold-Formed Steel Structures Library, 1983.
[17] Yu, Wei-Wen. Cold-formed steel design. John Wiley & Sons, 2000.
[18] Bejan A, Lorente S. Design with Constructal Theory, John Wiley & Sons, Inc, Hoboken, NJ, USA, 2008. https://doi.org/10.1002/9780470432709
[19] Bejan A, Lorente S. Constructal law of design and evolution: Physics, biology, technology, and society, Journal of Applied Physics, 2013; 113(15): 6. https://doi.org/10.1063/1.4798429
[20] Bejan A, Evolution in thermodynamics, Applied Physics Reviews, 2017; 4(1): 011305. https://doi.org/10.1063/1.4978611
[21] Miguel A F. Toward a quantitative unifying theory of natural design of flow systems: emergence and evolution. In: Constructal Law and the Unifying Principle of Design, Springer, New York, NY, USA, 2013: 21-39. https://doi.org/10.1007/978-1-4614-5049-8_2
[22] Lorenzini G, Biserni C, Estrada E, Isoldi LA, Dos Santos ED, Rocha LAO. Constructal design of convective Y-shaped cavities by means of genetic algorithm, Journal of Heat Transfer, 2014; 136(7): 071702. https://doi.org/10.1115/1.4027195
[23] Gonzales GV, Estrada ESD, Emmendorfer LR, Isoldi LA, Xie G, Rocha LAO, et al. A comparison of simulated annealing schedules for constructal design of complex cavities intruded into conductive walls with internal heat generation, Energy, 2015; 93: 372-382. https://doi.org/10.1016/j.energy.2015.09.058
[24] Ansys, User's manual (version 10.0), 2005.

[25] Madenci E, Guven I. The Finite Element Method and Applications in Engineering Using Ansys, Springer, New York, NY, USA, 2006.
[26] El-Sawy KM, Nazmy AS, Martini MI. Elasto-plastic buckling of perforated plates under uniaxial compression, Thin-Walled Structures, 2004; 42(8): 1083-1101. https://doi.org/10.1016/j.tws.2004.03.002
[27] Helbig D, Silva CCCD, Real MDV, Santos EDD, Isoldi LA, Rocha LAO. (2016). Study About Buckling Phenomenon in Perforated Thin Steel Plates Employing Computational Modeling and Constructal Design Method. Latin American Journal of Solids and Structures, 2016; 13(10); 1912-1936. https://doi.org/10.1590/1679-78252893
[28] Bejan A, Zane J P. Design in nature. Mechanical Engineering, 2012; 134(6); 42.